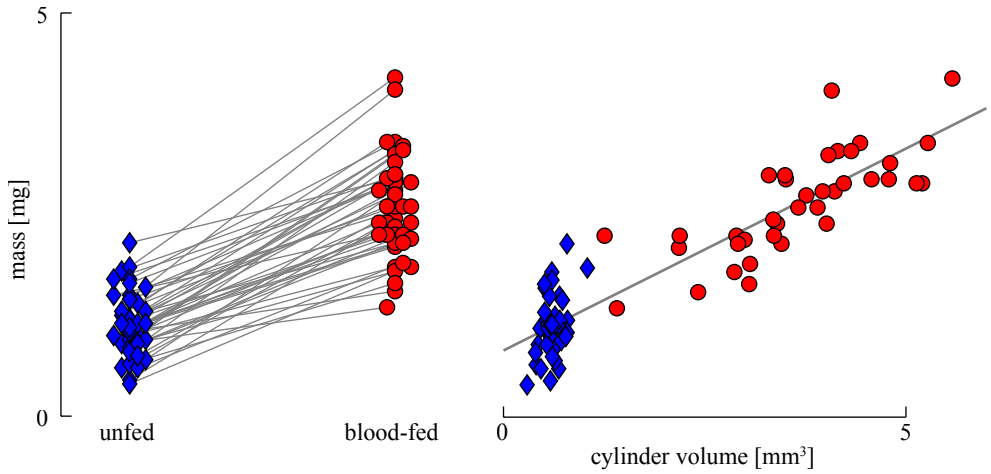

Fig. S1. Body mass was estimated based on the size of the mosquito, expressed by the cylindrical volume metric (Eqn. 1). (A) mass of all 44 measured mosquitoes before and after blood feeding. (B) correlation between body mass and the cylindrical volume metric for all mosquitoes, as described by the grey trend line (Eqn. 2). In both panels, blue diamonds are for mosquitoes before blood feeding, and red circles refer to post-blood feeding.

Table S1. Incentive (voluntary take-off or substrate vibration stimulus) did not significantly affect kinematics or force production during the take-off.

parameter	condition	incentive	n	mean	standard deviation	median	Q1	Q3	normality *p*-value	incentive *p*-value
Mass ratio (Rm) [-]	unfed	voluntary	15	1.01	0.05	1.00	0.97	1.04	0.908	0.737
		stimulus	16	0.99	0.08	1.01	0.95	1.01	0.812	
	blood-fed	voluntary	17	1.92	0.35	1.85	1.78	1.97	<0.001	0.406
		stimulus	15	1.95	0.28	1.90	1.79	2.12	0.868	
Push-off time ($\Delta t_{push\text{-}off}$) [ms]	unfed	voluntary	15	26.0	11.4	22.1	20.9	26.9	<0.001	0.953
		stimulus	16	26.5	11.9	22.6	19.3	28.7	0.001	
	blood-fed	voluntary	17	37.5	17.0	30.1	25.8	42.3	0.005	0.113
		stimulus	15	28.7	8.1	29.0	23.2	30.8	0.055	
Lift-off displacement ($X_{lift\text{-}off}/l_{body}$) [-]	unfed	voluntary	15	0.94	0.51	0.73	0.68	1.07	<0.001	0.441
		stimulus	16	0.78	0.28	0.73	0.61	0.88	<0.001	
	blood-fed	voluntary	17	0.99	0.32	0.92	0.86	1.06	0.024	0.054
		stimulus	15	0.80	0.33	0.76	0.57	0.93	0.095	
Lift-off speed ($U_{lift\text{-}off}$) [m s^{-1}]	unfed	voluntary	15	0.26	0.06	0.25	0.23	0.30	0.835	0.464
		stimulus	16	0.24	0.04	0.25	0.20	0.27	0.766	
	blood-fed	voluntary	17	0.21	0.04	0.22	0.18	0.23	0.200	0.122
		stimulus	15	0.19	0.06	0.18	0.15	0.22	0.371	
Lift-off ascent angle ($\gamma_{lift\text{-}off}$) [-]	unfed	voluntary	15	48°	12°	51°	43°	58°	0.028	0.540
		stimulus	16	52°	21°	55°	32°	70°	0.552	
	blood-fed	voluntary	17	34°	25°	40°	7°	54°	0.061	0.650
		stimulus	15	39°	23°	39°	22°	56°	0.927	
Lift-off body pitch ($\beta_{lift\text{-}off}$) [-]	unfed	voluntary	15	13°	18°	17°	4°	29°	0.131	0.890
		stimulus	16	13°	20°	21°	-4°	29°	0.315	
	blood-fed	voluntary	17	25°	13°	29°	20°	33°	0.001	1.000
		stimulus	15	25°	15°	25°	17°	38°	0.610	
Push-off force ($F/mg_{push\text{-}off}$) [-]	unfed	voluntary	15	2.08	0.40	2.06	1.87	2.29	0.423	0.395
		stimulus	16	1.98	0.46	1.94	1.71	2.23	0.605	
	blood-fed	voluntary	17	1.54	0.30	1.64	1.21	1.77	0.030	0.850
		stimulus	15	1.58	0.26	1.50	1.39	1.82	0.775	
Maximum push-off force ($F/mg_{push\text{-}off}$) [-]	unfed	voluntary	15	2.43	0.43	2.44	2.18	2.70	0.919	0.828
		stimulus	16	2.48	0.44	2.41	2.24	2.61	0.152	
	blood-fed	voluntary	17	2.00	0.45	2.14	1.62	2.34	0.169	0.910
		stimulus	15	2.03	0.36	2.06	1.81	2.24	0.297	
Aerial flight speed (U_{aerial}) [m s^{-1}]	unfed	voluntary	15	0.34	0.09	0.35	0.25	0.42	0.376	0.395
		stimulus	16	0.37	0.11	0.37	0.28	0.46	0.988	
	blood-fed	voluntary	17	0.36	0.07	0.39	0.30	0.40	0.368	0.308
		stimulus	15	0.34	0.08	0.32	0.27	0.41	0.177	
Aerial ascent angle (γ_{aerial}) [-]	unfed	voluntary	15	30°	16°	36°	25°	42°	0.026	0.093
		stimulus	16	21°	21°	24°	1°	33°	0.634	
	blood-fed	voluntary	17	17°	17°	17°	6°	29°	0.971	0.546
		stimulus	15	13°	22°	-2°	-4°	35°	0.006	
Aerial body pitch (β_{aerial}) [-]	unfed	voluntary	15	26°	24°	39°	12°	43°	0.038	0.243
		stimulus	16	20°	20°	26°	1°	34°	0.028	
	blood-fed	voluntary	17	31°	15°	33°	27°	42°	0.037	0.571
		stimulus	15	28°	18°	29°	13°	45°	0.341	
Aerial force (F/mg_{aerial}) [-]	unfed	voluntary	15	1.05	0.11	1.03	0.98	1.10	0.827	0.859
		stimulus	16	1.06	0.15	1.02	0.98	1.10	0.039	
	blood-fed	voluntary	17	1.10	0.11	1.12	1.01	1.14	0.219	0.910
		stimulus	15	1.03	0.09	1.05	1.00	1.09	0.109	

Table S2. The effect of blood-feeding on body mass, and on the take-off dynamics and force production throughout the complete take-off.

parameter	feeding condition	n	mean	standard deviation	median	Q1	Q3	normality *p*-value	feeding condition *p*-value
Mass ratio (R_m) [-]	unfed	31	1.00	0.06	1.01	0.97	1.04	0.867	**0.010**
	blood-fed	32	1.93	0.32	1.88	1.80	2.02	**<0.001**	
Push-off time ($\Delta t_{push\text{-}off}$) [ms]	unfed	31	26.3	11.5	22.6	19.6	27.4	**<0.001**	**0.002**
	blood-fed	32	33.4	14.1	29.3	25.3	36.4	**<0.001**	
	all	63	29.9	13.3	26.0	21.3	32.2	-	-
Lift-off displacement ($X_{lift\text{-}off}/l_{body}$) [-]	unfed	31	0.86	0.41	0.73	0.65	0.89	**<0.001**	0.159
	blood-fed	32	0.90	0.33	0.89	0.69	0.98	**0.023**	
	all	63	0.88	0.37	0.80	0.67	0.93	-	-
Lift-off speed ($U_{lift\text{-}off}$) [m s^{-1}]	unfed	31	0.25	0.05	0.25	0.21	0.28	0.454	**0.001**
	blood-fed	32	0.20	0.05	0.21	0.16	0.23	0.500	
	all	63	0.23	0.05	0.23	0.19	0.26	-	-
Lift-off ascent angle ($\gamma_{lift\text{-}off}$) [-]	unfed	31	50°	17°	53°	35°	60°	0.493	**0.016**
	blood-fed	32	36°	24°	39°	15°	55°	0.221	
Lift-off body pitch ($\beta_{lift\text{-}off}$) [-]	unfed	31	13°	19°	19°	-2°	29°	**0.045**	**0.010**
	blood-fed	32	25°	14°	28°	18°	34°	**0.026**	
Push-off force ($F/mg_{push\text{-}off}$) [-]	unfed	31	2.03	0.43	1.97	1.75	2.29	0.277	**0.008**
	blood-fed	32	1.56	0.28	1.57	1.37	1.77	**0.049**	
Maximum push-off force ($F/mg_{push\text{-}off,\ max}$) [-]	unfed	31	2.46	0.43	2.44	2.21	2.63	0.249	**0.030**
	blood-fed	32	2.01	0.41	2.10	1.71	2.27	0.160	
	all	63	2.23	0.47	2.23	2.01	2.48	-	-
Aerial flight speed (U_{aerial}) [m s^{-1}]	unfed	31	0.36	0.10	0.36	0.27	0.43	0.953	0.853
	blood-fed	32	0.35	0.07	0.35	0.29	0.41	0.133	
Aerial ascent angle (γ_{aerial}) [-]	unfed	31	26°	19°	31°	9°	40°	0.134	**0.035**
	blood-fed	32	15°	19°	12°	-3°	30°	0.064	
Aerial body pitch (β_{aerial}) [-]	unfed	31	23°	22°	27°	6°	40°	**0.013**	0.219
	blood-fed	32	30°	16°	32°	22°	44°	**0.040**	
Aerial force (F/mg_{aerial}) [-]	unfed	31	1.05	0.13	1.03	0.98	1.10	**0.033**	0.251
	blood-fed	32	1.07	0.10	1.08	1.00	1.13	0.136	

Table S3. The effect of blood-feeding on wingbeat kinematics during the aerial phase of the take-off.

parameter	feeding condition	n	mean	standard deviation	median	Q1	Q3	normality *p*-value	feeding condition *p*-value
Wingbeat frequency (f) [Hz]	unfed	29	579	38	584	555	603	0.505	0.534
	blood-fed	29	573	37	582	543	594	0.635	
Stroke amplitude (A_{stroke}) [-]	unfed	29	42°	5°	42°	39°	46°	0.473	**<0.001**
	blood-fed	29	54°	6°	56°	50°	59°	0.268	
Pitch amplitude (A_{pitch}) [-]	unfed	29	121°	10°	122°	114°	129°	0.692	**<0.001**
	blood-fed	29	134°	12°	135°	124°	139°	0.614	
Stroke-plane pitch adjustment (σ) [-]	unfed	29	-1°	4°	-1°	-4°	1°	0.221	**<0.001**
	blood-fed	29	-9°	4°	-9°	-12°	-5°	0.130	

Table S4. The relative contribution of leg-derived push-off forces and wing-derived aerodynamic forces to total force production during the push-off phase and aerial phase of the take-off.

parameter	feeding condition	n	mean	standard deviation	median	Q1	Q3	normality *p*-value	feeding condition *p*-value
Push-off force ($F/mg_{push\text{-}off}$) [-]	total force	16	2.04	0.41	1.92	1.75	2.36	0.236	**<0.001**
	aerodynamic	16	1.13	0.42	0.98	0.83	1.39	0.066	
Aerial force (F/mg_{aerial}) [-]	total force	16	1.18	0.19	1.17	1.00	1.39	0.093	0.136
	aerodynamic	16	1.14	0.41	1.05	0.87	1.18	**<0.001**	
Force ratio (F_{aero}/F_{leg}) [-]	unfed	8	2.13	1.64	1.70	1.00	3.00	0.086	0.105
	blood-fed	8	0.96	0.24	0.91	0.76	1.20	0.269	
	all	16	1.55	1.29	1.20	0.76	1.71	-	-

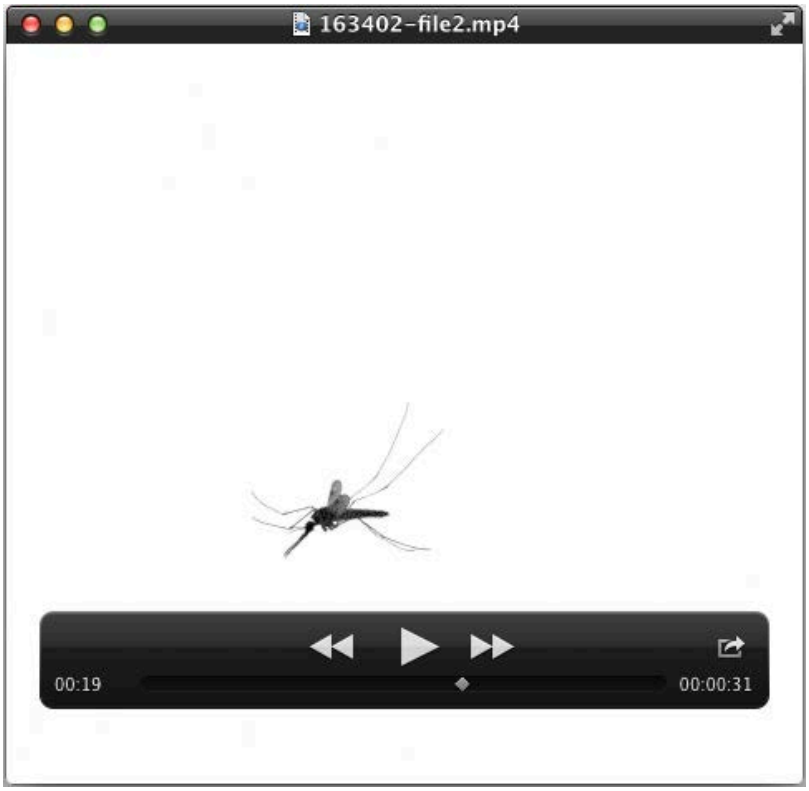

Movie 1. High-speed video of the take-off of an unfed mosquito filmed from the side. The video was recorded at 13,500 frames per second, and play-back was slowed down 450 times. The video corresponds to the photo-montage of Fig. 2A.

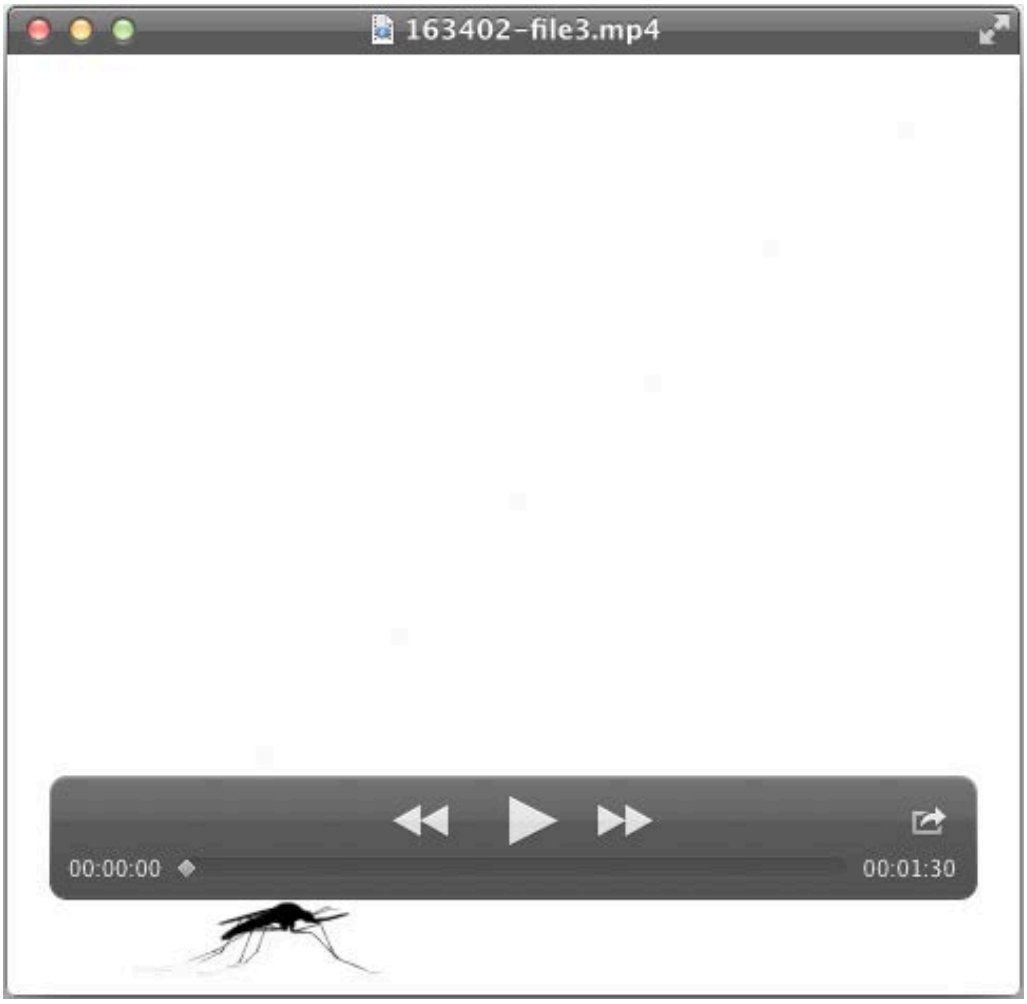

Movie 2. High-speed video of the take-off of an unfed mosquito filmed from the side. The video was recorded at 13,500 frames per second, and play-back was slowed down 450 times. The video corresponds to the photo-montage of Fig. 2B.

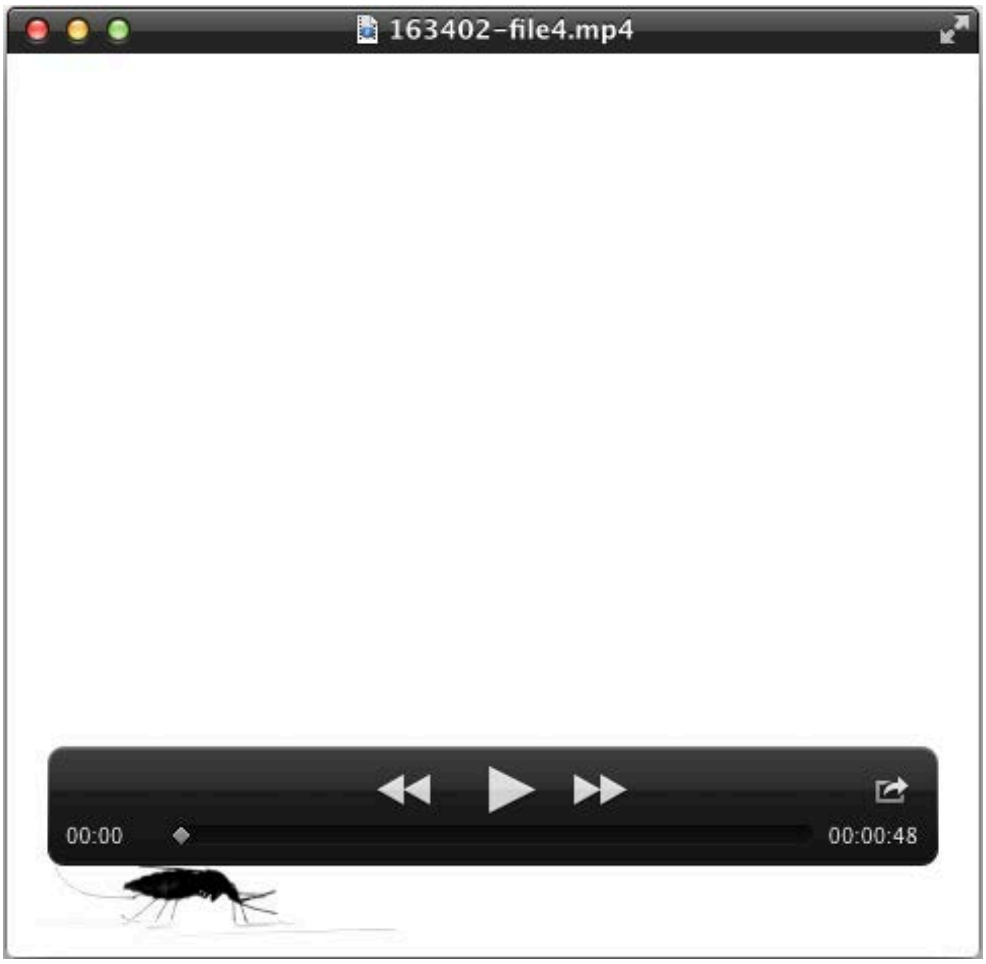

Movie 3. High-speed video of the take-off of a blood-fed mosquito filmed from the side. The video was recorded at 13,500 frames per second, and play-back was slowed down 450 times. The video corresponds to the photo-montage of Fig. 2C.

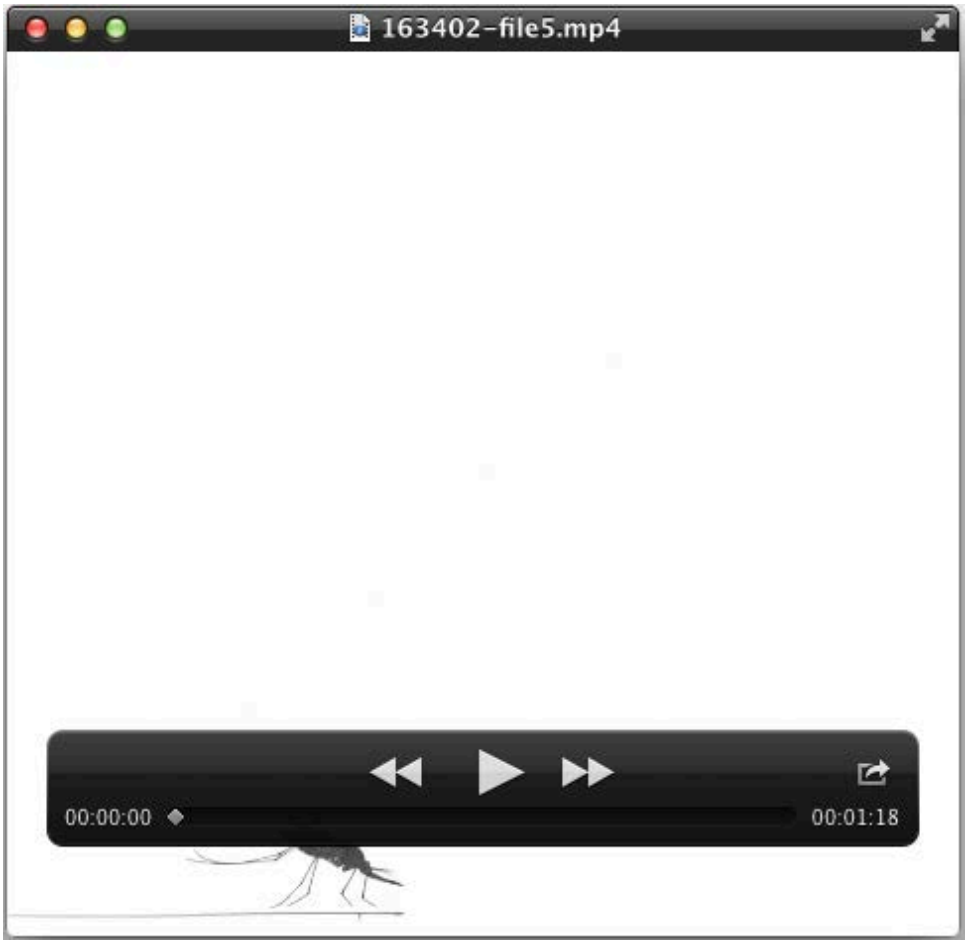

Movie 4. High-speed video of the take-off of a blood-fed mosquito filmed from the side. The video was recorded at 13,500 frames per second, and play-back was slowed down 450 times. The video corresponds to the photo-montage of Fig. 2D.

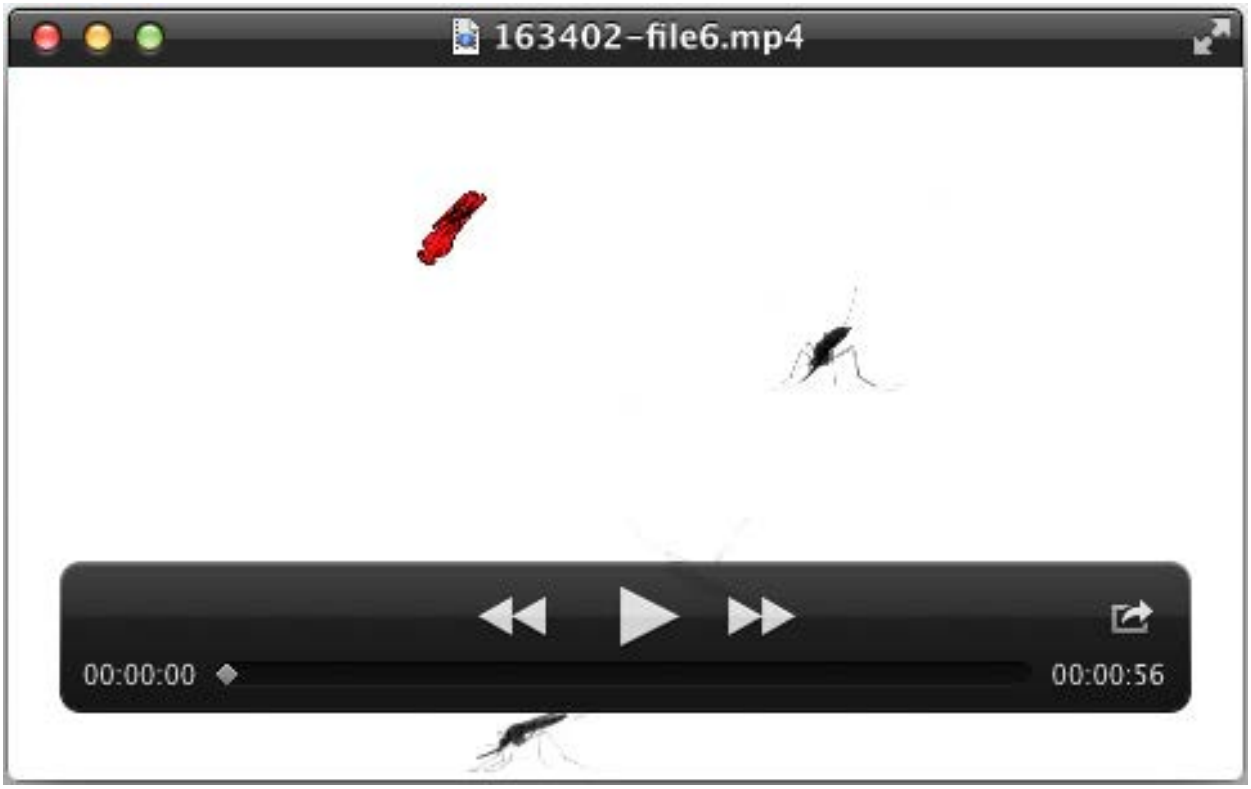

Movie 5. High-speed video and 3D model reconstruction from video tracking for the unfed mosquito of Fig. 5A-D. The movie consists of the front view video (top right), side view video (bottom left), top view video (bottom right), and the 3D model reconstruction (top left). The mosquito model consists of a rigid body and two rigid wings. The videos were recorded at 13,500 frames per second, and play-back was slowed down 450 times.

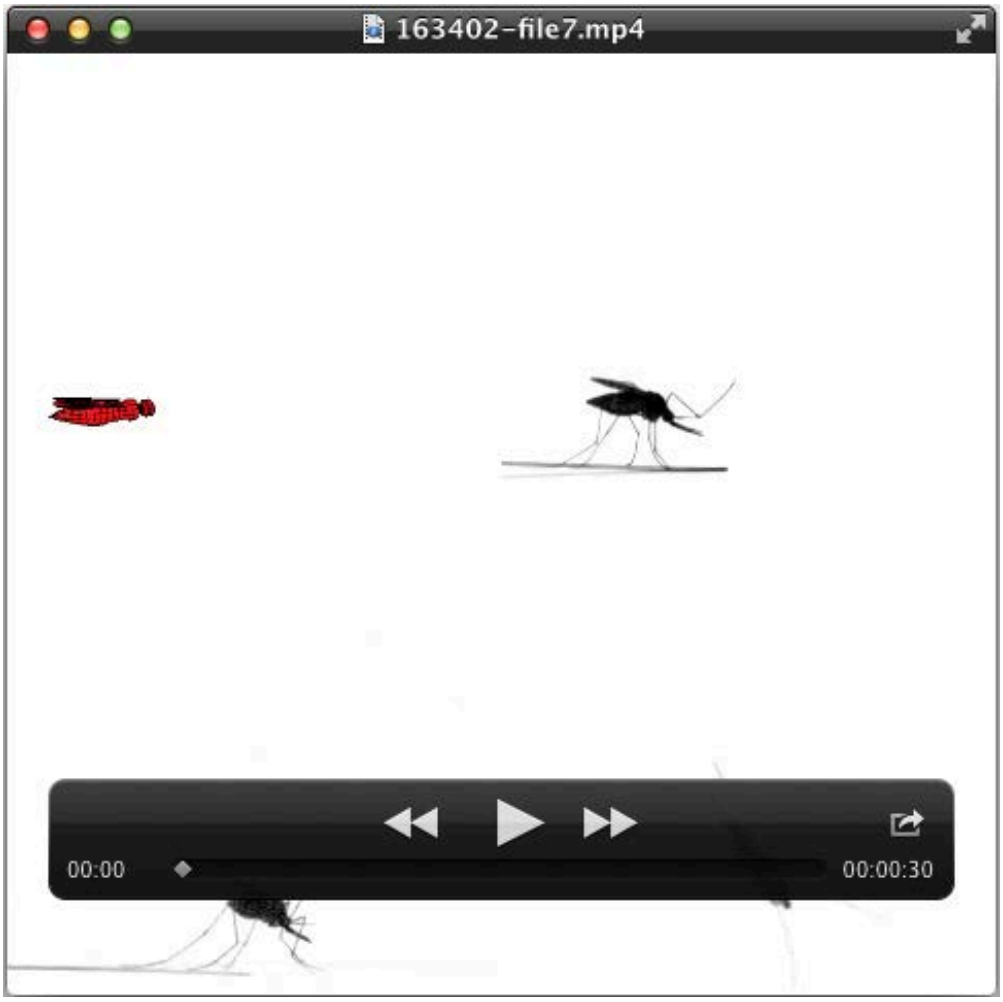

Movie 6. High-speed video and 3D model reconstruction from video tracking for the blood-fed mosquito of Fig. 5F-I. The movie consists of the two perpendicular side view videos (top right and bottom left), top view video (bottom right), and the 3D model reconstruction (top left). The mosquito model consists of a rigid body and two rigid wings. The videos were recorded at 13,500 frames per second, and play-back was slowed down 450 times.

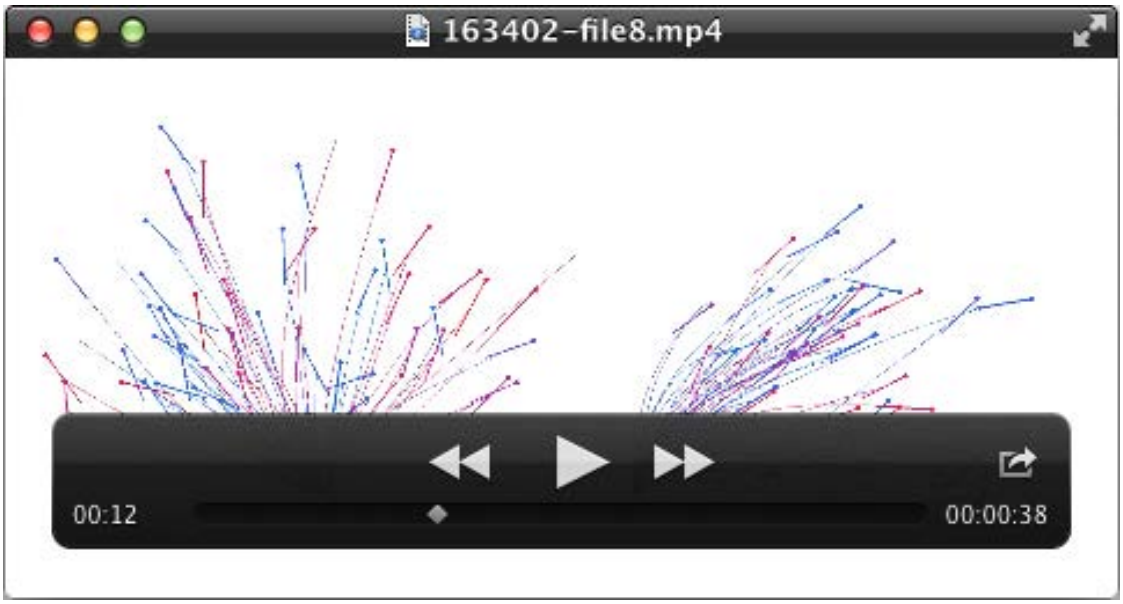

Movie 7. Top view (left) and side view (right) of the take-off dynamics of all experimental mosquitoes, corresponding to Fig. 3A,B. The trajectories were overlaid such that all lift-offs occurred at the same time. Thin lines show flight trajectories, and lollypops show the orientation of the longitudinal body axis, whereby the circles indicate head position, and stick length represents body length. The take-off dynamics is slowed down 100 times. Trajectories are color-coded with body weight according to the color-bar in Fig. 3B.

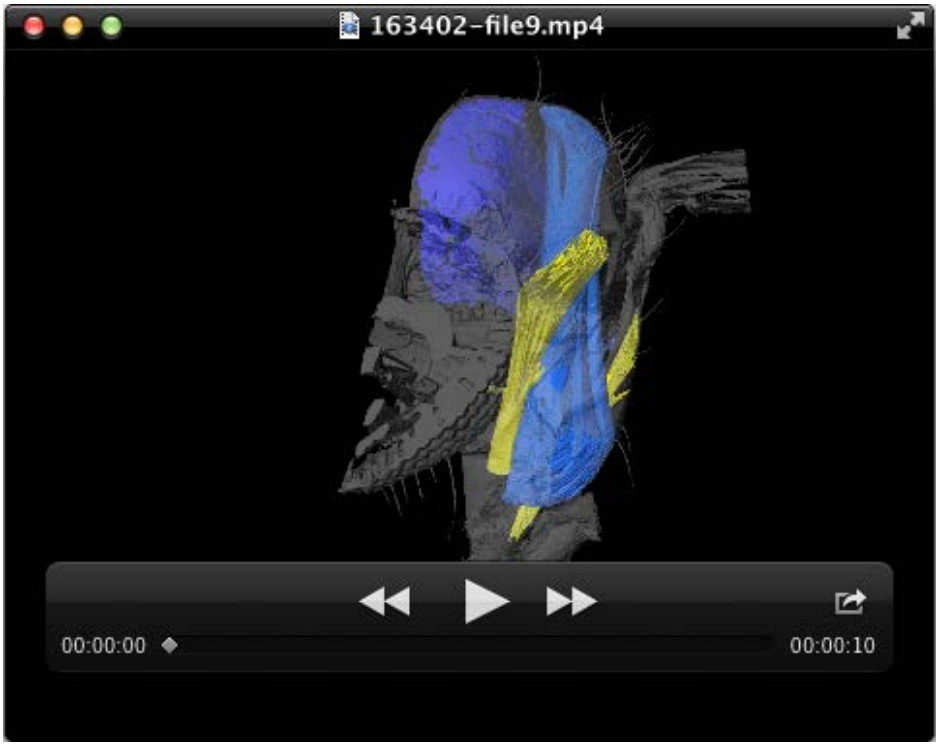

Movie 8. Three-dimensional μCT reconstruction of the muscular system within the left half of the thorax of a female malaria mosquito, as also shown in Fig. 6. The indirect flight power muscles consist of the dorso-ventral muscles (in light blue) and the dorso-longitudinal muscles (in dank blue). The leg muscles that mostly power push-off are the extracoxal depressor muscles of the trochanter of the front, middle and hind leg (in yellow). Surrounding material that was stained but did not belong to the segmented muscles was visualized in transparent grey.